Direct Observations of the Mechanical Behaviors of the Cytoskeleton in Living Fibroblasts

Steven R. Heidemann,‡ Stefanie Kaech,* Robert E. Buxbaum,‡ and Andrew Matus*

*Friedrich Miescher Institute, Basel CH-4002, Switzerland; and ‡Department of Physiology, Michigan State University, East Lansing, Michigan 48824-1101

Abstract. Cytoskeletal proteins tagged with green fluorescent protein were used to directly visualize the mechanical role of the cytoskeleton in determining cell shape. Rat embryo (REF 52) fibroblasts were deformed using glass needles either uncoated for purely physical manipulations, or coated with laminin to induce attachment to the cell surface. Cells responded to uncoated probes in accordance with a three-layer model in which a highly elastic nucleus is surrounded by cytoplasmic microtubules that behave as a jelly-like viscoelastic fluid. The third, outermost cortical layer is an elastic shell under sustained tension. Adhesive, laminin-coated needles caused focal recruitment of actin filaments to the contacted surface region and increased the cortical layer stiffness. This direct visualization of actin recruitment confirms a widely postulated model for mechanical connections between extracellular matrix proteins and the actin cytoskeleton. Cells tethered to laminin-treated needles strongly resisted elongation by actively contracting. Whether using uncoated probes to apply simple deformations or laminin-coated probes to induce surface-to-cytoskeleton interaction we observed that experimentally applied forces produced exclusively local responses by both the actin and microtubule cytoskeleton. This local accomodation and dissipation of force is inconsistent with the proposal that cellular tensegrity determines cell shape.

Key words: cytoskeleton • cytomechanics • biorheology • integrins • cell shape

TAGGING proteins with green fluorescent protein (GFP)[1] provides a new means of directly observing the cytoskeletal elements in living cells (Ludin and Matus, 1998). We exploited this new methodology to study the mechanical behaviors of the actin and microtubule (MT) cytoskeletons of fibroblasts subjected to various deformations. The mechanical responses of polymeric materials to deformation has long been an active area of investigation in engineering, physics, and biology (Ferry, 1959). In biology, the main focus is on cell shape and motility (Taylor and Condeelis, 1979; Bereiter-Hahn et al., 1987; Elson, 1988; Stossel, 1993; Hochmuth, 1993) with the aim of identifying the physical properties and roles of the cytoskeleton that support these functions (e.g., Sato et al., 1983, 1987; Buxbaum et al., 1987; Elson, 1988; Janmey et al., 1994). One of the important goals of such work is to understand how the behaviors of the individual polymer molecules relate to the structure and physical activities of the cell.

Rheological measurements on whole cells and on cytoskeletal filaments in vitro have relied on applying forces or deformations and analyzing their interrelationships based on a variety of Newtonian (e.g., Valberg and Albertini, 1985; Evans and Yeung, 1989; Tran-Son-Tay et al., 1991) and non-Newtonian (e.g., Peterson et al., 1982; Dong et al., 1991; Adams, 1992; Thoumine and Ott, 1997) assumptions about the flow fields produced. This approach has produced widespread agreement on some aspects of cellular rheology such as the presence of an elastic cell cortex that surrounds a primarily fluid cytoplasm. However, there is wide disagreement for the values of elastic constants and viscosities caused in part by the differing cell types, rheological methods, and assumptions employed. Proposals for the relationships between cytoskeletal structure and cellular mechanics range from simple continuum models (Dong et al., 1991; Hochmuth, 1993) to complex tensegrity structures in which actin forms an integrated tensile network supported by compressive MT struts or attachments to the substratum (Heidemann and Buxbaum, 1990; Ingber, 1997) and models in which the cytoskeleton forms a percolation structure through the cytoplasm (Forgacs, 1995). Without visualization of the cyto-

The first two authors contributed equally to this paper.

Address correspondence to Dr. Heidemann, Department of Physiology, Michigan State University, East Lansing, MI 48824-1101. Tel.: (517) 355-6475, ext. 1236. Fax: (517) 355-5125. E-mail: heidemann@psl.msu.edu

1. *Abbreviations used in this paper:* GFP, green fluorescent protein; MT, microtubule.

skeleton, it is unlikely that rheological experiments will be able to distinguish among these models or assess how the underlying cytoskeleton behaves and is organized to produce other cellular mechanical behaviors.

Through GFP technology, we were able to directly observe the fluid and elastic motions of actin and MTs of living fibroblasts in response to simple but informative deformations. We were able to observe flow fields and the motion of individual polymer molecules and multipolymer structures such as bundles. The cytoskeleton responded with only highly localized responses to applied forces and deformations and we found little evidence for interconnections among cytoskeletal elements or cellular layers. Further, observations of well-spread fibroblasts and cells in the process of spreading indicate that the degree of substratum attachment does not substantially affect the mechanics of fibroblasts.

Materials and Methods

GFP Constructs

The COOH-terminal fusion construct of the cDNA for the MT-associated protein MAP2 with GFP cDNA has been described earlier (Kaech et al., 1996). The fusion construct of the cDNA for mouse β6-tubulin isoform (kind gift of N. Cowan, New York University, New York) with the coding sequence of EGFP (Clontech) was constructed analogously into a beta-actin driven expression vector (Ludin et al., 1996). Plasmids were purified using Qiagen columns.

Cell Culture And Transfection

The rat embryo fibroblast cell line REF 52 was grown under standard conditions in DME supplemented with 10% FCS (Life Technologies). Cells were plated onto 18-mm round glass coverlips 14–20 h before transfection. Cultures were transfected using lipofectamine (Life Technologies) or Fugene 6 (Roche Diagnostics) according to the manufacturer's instructions.

Both well-spread and rounded cells were manipulated. Well-spread cells came from cultures that had been transfected and plated some 24–72 h before experimentation. Rounded, spreading cells were obtained by replating cells that had been transfected 24–72 h earlier and manipulating them 2–6 h after replating. To induce retraction of cell edges in well-spread cells, cells were incubated on the microscope stage in Ca- and Mg-free PBS supplemented with 0.1 or 0.5 mM EDTA to chelate extracellular Ca and Mg ions resulting in a rounding of cells within 10–30 min.

Microscopy

For live imaging, coverslips were mounted in observation chambers (Type 1; Life Imaging Services) in a special formula of DME with 1/10 of regular riboflavin content (Life Technologies) and imaged at 37°C on a Leica DM-IRBE inverted fluorescence microscope equipped with high numerical aperture oil lenses (Leica) and a GFP-optimized filter set (Chroma Technology). Images were captured using either a Kappa CF8/1 DXC (Kappa) or a MicroMax (Princeton Instruments) cooled CCD camera and MetaMorph Imaging Software (Universal Imaging Corporation). Figures were assembled with Adobe Photoshop and Illustrator.

Mechanical Deformations and Force Measurements

Cells were deformed by poking and prodding them with glass needles that had been calibrated to determine their bending constant, i.e., their resistance to deflection. The fabrication and calibration of needles has been described in detail (Heidemann et al., 1999) and they have been used routinely to apply tension to cultured neurons (Dennerll et al., 1989; Lamoureux et al., 1992; Chada et al., 1997). In brief, two needles were mounted in a micromanipulator; one needle was calibrated for its bending constant and used as the needle applied to the cell, while the other needle was used as an unloaded reference for bending of the calibrated needle and for possible drift of the micromanipulator system. The bending constants of the calibrated needles were between 10–30 μdyne/μm and some needles were pretreated with 0.1% polylysine and/or 50 μg/ml laminin to promote adhesion. Because of the high-magnification, high-NA objectives used to visualize GFP-tagged proteins in the cell and the high forces often applied to or exerted by REF 52 cells, it was not possible to keep both calibrated and reference needle within the digitized image frame captured by the computerized microscopy system. Instead, the bending of the calibrated needle was measured in real time from its deflection distance (relative to the reference needle) using an ocular reticle that had been calibrated with a stage micrometer.

Results

The Nuclear Region and Actin-rich Peripheral Regions Are Generally Elastic

The nuclei of REF cells as well the actin cytoskeleton show almost purely elastic behavior in response to all manipulations that deformed their arrangement or shape. Fig. 1 shows an example in which the manipulating needle was poked into the nuclear region of a REF cell transfected with GFP–γ-actin, causing a sharp deformation of the nucleus and an accumulation of perinuclear actin at the tip of the needle. Actin not in the path of the needle showed no significant change in organization. After holding the deformation for ~1 min, the needle was released (01:00). In this and other examples the nucleus behaved as a viscoelastic solid with an initial rapid phase of elastic recovery of most of its original shape (01:00 to 01:34) followed by a slower, apparently damped approach to original shape (02:52). Indeed, this behavior is qualitatively similar to a spring-and-dashpot model for neurite elasticity of cultured neurons (Dennerll et al., 1989). Nevertheless, we observed some net movement of actin and nucleus. For example, the arrows in Fig. 1 mark the initial position of the nucleus. As can be seen, the nucleus and its surrounding actin halo shifted somewhat in the direction of the experimentally applied force. As shown in Fig. 1, we routinely observed that the nucleus and its surrounding GFP-actin network behaved coordinately when the nucleus was displaced.

In elongated cells, where it was possible to deform the cell and the underlying cytoskeleton without deforming the nucleus, we observed that the actin cytoskeleton of the peripheral cytoplasm was also highly elastic. Fig. 2 shows an example in which an elongated REF cell transfected with GFP–γ-actin was subjected to a substantial deformation in the middle of an actin bundle along a concave webbed edge, which has been postulated to support part of the tension of cell adhesion (Zand and Albrecht-Buehler, 1989). The induced deformations quickly recovered after release of the needle. This recovery was particularly impressive in that movement of the needle caused a small nick in the actin at the cell edge before the manipulation. It can be seen that this cut severed some actin filaments, in turn opening a gap in the margin of the cell. This indicates the margin is under tension, as expected. Further, the major deformation also clearly damaged the cell, causing parting of the cell immediately after elastic recovery. The damage sustained by the cell would be expected to dissipate part of the tension load, and thus act to suppress at least part of any elastic behavior. Complete elastic recovery by the actin cytoskeleton in the face of a dissipating influence was unexpected.

We extended these observations of the elasticity and

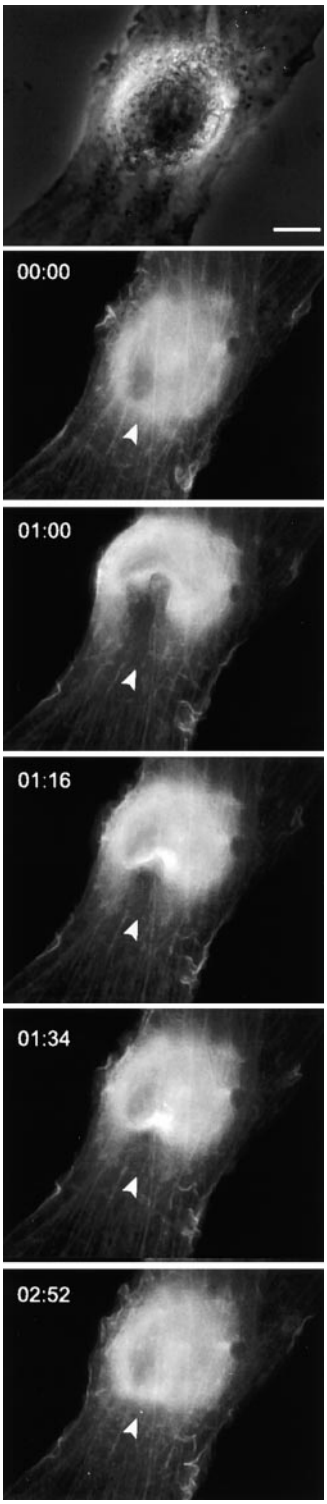

Figure 1. Elasticity of nucleus and perinuclear actin (min:s). Bar, 15 μm. (00:00) Phase and fluorescent images of GFP–γ-actin–transfected cell just before poking with a needle. The arrowhead in the fluorescent frames shows the initial position of the edge of the nucleus. (01:00) Needle is inserted and held for 1 min and removed completely from the cell immediately after this image. (01:16) Approximately half the initial deformation has recovered in 16 s. (01:34) Further recovery 30 s after needle removal. (02:52) Note from the arrowhead that while the nucleus has substantially recovered it's shape, it has changed location slightly in the cytoplasm.

sustained tension on the actin network by manipulations specifically intended to sever the cytoskeleton. Microneedles were broken off 1–2 mm from the tip and the sharp, broken glass edge of such needles were then used as a microknife to cut into a cell, severing the cytoskeletal filaments in a local region of cytoplasm. Fig. 3 A shows a cell transfected with GFP–γ-actin subjected to a small nick at 0:07, again made in the middle of an actin bundle along a concave webbed edge. After this small cut, the needle was withdrawn completely. The images on the right side of the figure are difference images created by subtracting the pixels of the fluorescent image to the left with the next earlier image shown in the figure. As shown by both the fluorescent images to the left and the difference images to the right, the actin bundle retracts ~12 μm on either side of the cut, indictating both tension and elasticity by the severed actin bundle. However, the difference images show that the effect of this release of tension was highly local: there is essentially no change in any other fluorescent actin bundle. Indeed, what appears to be a part of the severed actin bundle, extending toward the lower right corner of the cell, also shows little or no change in position for ~1 min after. Fig. 3 B shows that the severed edge itself continued to remain stable for several minutes after the cut was made. However, 3–4 min after making the cut the entire right hand portion of the cell was observed to contract in a manner suggestive of increased tension on a catenary (e.g., pulling on the ropes of a simple rope suspension bridge). As shown by the difference image of Fig. 3 B, the cut edge of the cell increased slightly in diameter (i.e., the linear distance along the edge declined slightly) while the opposite, uncut cell edge moved in the same direction, e.g., as would the roadway suspended from the tightened rope suspension bridge. We presume that this cellular contraction was an active response to the cutting.

The Cytoplasmic Microtubule Network Shows Fluid Behaviors

Two GFP-tagged probes were used to visualize MTs. Transfection with GFP-tubulin works directly by incorporation of the fluorescent protein into the MT lattice. Microtubules were also visualized with GFP-MAP2c, a neuronal protein that binds to the outside of the lattice. Both probes have advantages and disadvantages. Despite the addition of the GFP component, GFP-tubulin does not appear to disturb MT structure or dynamics (Kaech et al., 1996; Ludin and Matus, 1998). It also seems unlikely that it would alter the MT array of the cell because cells have a translational-stage feedback mechanism that regulates the concentration of free tubulin subunits (Cleveland, 1988). Although this is advantageous for moderating the level of GFP-tubulin expression, it has the disadvantage that the labeled MTs are often too dimly fluorescent to visualize effectively. MAP2c is a well-characterized, high molecular weight, MT-associated protein of neurons that binds with high affinity to MTs (Matus, 1994). Expression and overexpression of this protein, labeled with GFP, in non-neural cells does not materially affect the dynamics of MTs (Kaech et al., 1996), and results in a relatively large number of cells with brightly fluorescent MTs. Like MAP2c itself, however, GFP-MAP2c does cause bundling of MTs in those cells in which it is particularly highly expressed (Weisshaar et al., 1992; Kaech et al., 1996). We noted no differences in the mechanical behaviors of the cellular MT array between cells transfected with GFP-tubulin or GFP-MAP2c.

In contrast to the elasticity of the actin cytoskeleton, the MT-based cytoskeleton when visualized with either probe recovered slowly from deformations and showed some de-

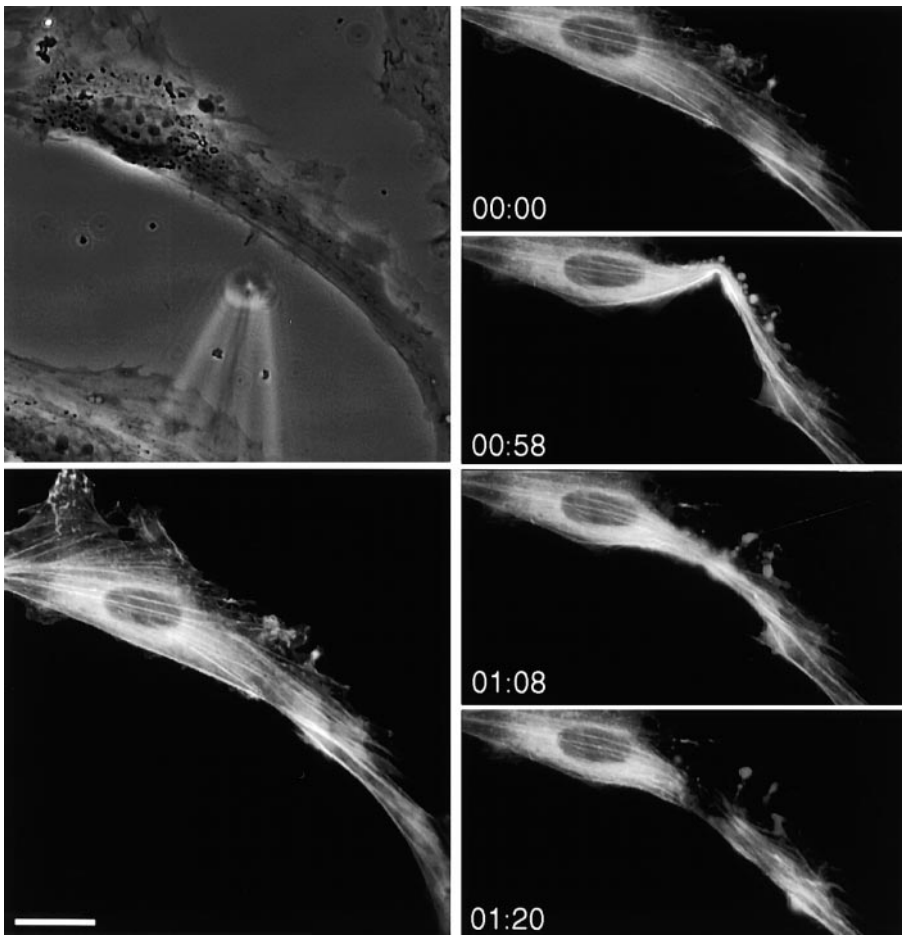

Figure 2. Elasticity of actin in spread regions of the cell (min:s). Bar, 30 μm. Phase image: cell before any manipulation. During positioning, the needle nicked the edge of the cell producing a small tear in the outer actin network. (fluorescent image). (00:00) Cell immediately before poking by needle and held for ~1 min (00:58). Cell recovered elastically, like a stretched rubber band, within 10 s of needle removal. This elastic recovery occurred despite the damage to the cell sustained before the sharp deformation and apparently during the deformation, which causes the cell to sever at the site of deformation (01:20).

gree of permanent deformation (i.e., deformations that persisted for the time scale of these observations) or flow. Fig. 4 is a REF cell transfected with GFP-MAP2c that was sharply poked in the nuclear region, which was surrounded by three bundles of MTs. The needle penetrated through and parted the cytoplasm such that the substratum was revealed, but without damaging the cell. After release of the needle, the MTs remained parted for >5 min, slowly filling the space made by the needle. Further, comparison of the position and curvature of the three perinuclear MT bundles before deformation by the needle (00:09) with their geometry some 10 min after removal of the needle (14:33) show that these MTs have been displaced and remain displaced. Slow recovery after deformation and some degree of long-lasting displacement were typical of the response of GFP-illuminated MTs, whether via GFP-tubulin or GFP-MAP2.

We assessed the response of the MT cytoskeleton to cutting using broken needles as before. Fig. 5 shows a fibroblast transfected with GFP-tubulin in which a deep cut was made in the cytoplasm, approximately perpendicular to the MT array, beginning in a particularly small radius concave region of the cell (Fig. 5, 00:00, right panel). Initially, MTs collected into a bundle at the tip of the needle (Fig. 5, 00:16, left panel). Subsequently, the cell fragment on the right was disrupted and lysed within 1 min accompanied by depolymerization of the MTs in the fragment. However, the cut edge of the cell to the left of the needle path retained its integrity with little change in the MT array in this region or in the extent of cell spreading at this cut edge.

We confirmed the viscoelastic behavior of the MT cytoskeleton during substratum detachment and cell rounding of REF 52 cells transfected with GFP-tubulin. Cells that had been plated ~16 h earlier were stimulated to detach and round up by adding EDTA to a final concentration of 0.1–0.5 mM. Two behaviors were routinely observed during subsequent retractions from the substratum; buckling of MTs in regions undergoing rapid retractions (Fig. 6), and shearing flows in regions of slow retractions (Fig. 7). Fig 6 shows a sequence of a rapidly retracting cell. As shown in Fig. 6 B, the cone-shaped extension toward the lower left of the cell retracted 20 μm in 2 min 39 s. (between 00:21 and 3:00) and is accompanied by obvious buckling of the MTs within this region. Importantly, the MTs begin buckling as soon as the margin of the cell began retracting. For example, between 00:21 and 1:10, the extension retracted only 5 μm, but there is clear buckling of the MT bundle near 11 o'clock. Fig. 6 C shows that the right side of this same cell undergoes an even more catastrophic buckling of MTs in response to the collapse of adhesion in this region, where the upper region of cytoplasm shown in Fig. 6 C retracts 15 μm in 11 s (between 02:49 and 03:00). In this and all other cases of MTs bearing new

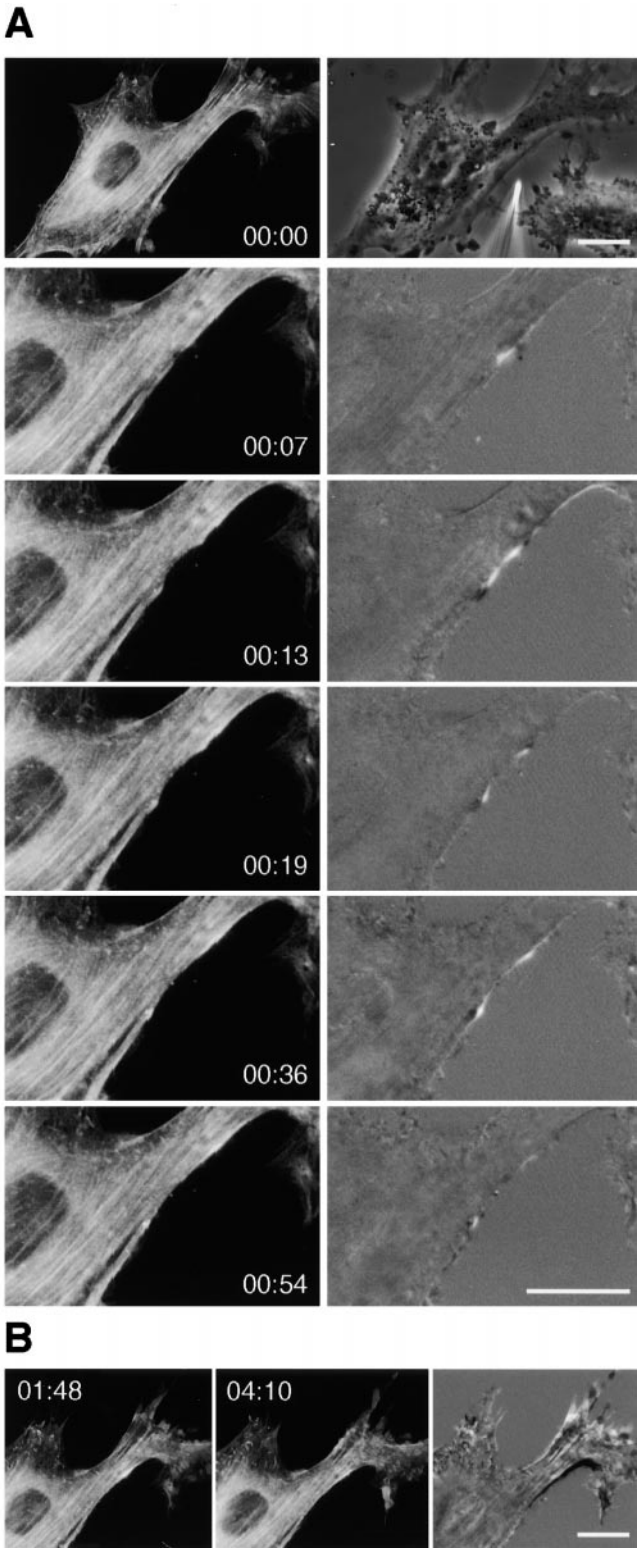

Figure 3. Short and long term behavior of GFP–γ-actin–transfected cell whose actin edge bundle was cut (min:s). Bars, 30 μm. (A) Short-term behavior after cut. (00:00) Lower magnification fluorescent and phase view of cell before any manipulation. (00:07–00:54) A nick was made in actin bundle with broken needle, which was immediately removed. Subsequently, this actin bundle moves away from the site of the cut in both directions over the next 20–30 s. The difference images seen on the right are pixel substractions of each fluorescent image on the left and its just earlier counterpart; regions increasing in pixel density are shown in black, those decreasing are shown in white. For example, the difference image of 00:13 is the fluorescent image at this time point subtracted from the fluorescent image of 00:07 and nearly all the change between the two images is concentrated 6 mm on either side of the site of the cut. Note that the difference images show little or no change in the actin fluorescence even in region directly neighboring the severed actin bundle. (B) Longer term behavior of the same cell as in A in response to the same small cut. (1:48–4:10) The severed actin bundle region remains stable but the "catenary" of the cell nicked at 00:07 contracts and reduces its radius of curvature on the cut side, while the back region moves along with it. This is better seen in the difference image to the extreme right, though it is even more clearly seen as a dynamic process.

compressive loads, there was no evidence for MT disassembly stimulated by compressive forces, although we clearly observed MT assembly/disassembly in this cell characteristic of MT dynamic instability.

Fig. 7 shows an example of a cell whose rounding up occurred more slowly. The lower region of the cell retracted 18 μm in 21 min accompanied primarily by shearing movements of MTs with only small amounts of buckling. Rounding up frequently occurs by a retraction of the MT-containing cytoplasm although the cell margin remains fully extended. Comparing the phase images in Fig. 7, A and E, taken 41 min apart, indicates that the MT array initially extended to the outer margin of the cell, which did not change position, but the MT-containing cytoplasm has retracted some 20 μm apparently within the still extended cell cortex.

Response of Fibroblasts to Towing Forces via Integrin-mediated Attachments

Integrin-mediated cell attachment to a substratum also mediates mechanical attachments to the cytoplasmic actin cortex and has been shown to play a major role in regulating cytoplasmic architecture, cell shape, and motility (Ingber, 1991; Hynes, 1992; Yamada and Miyamoto, 1995; Burridge et al., 1997). We examined the response of both the actin and the MT cytoskeleton to towing forces exerted by calibrated glass needles treated with laminin, an ECM protein known to bind to integrin molecules.

Calibrated laminin-treated glass needles were applied under moderate force (~200 μdynes) to the surface of REF cells transfected with GFP–γ-actin. In six separate experiments using different cells and different needles, we observed an accumulation of actin in the cortex beneath and surrounding the needle tip within minutes of applying the needle (e.g., Fig. 8, 01:00 and 02:00). If the needle was moved along the cell surface, applying forces <200 μdynes, the actin accumulation translocated with the needle. That is, moving the needle caused the accumulated actin to "walk" across the dorsal cell surface (Fig. 8). The attachment of laminin-treated needles to the cell surface is mechanically robust. In the example shown in Fig. 8, when the needle and actin reached the cell margin, a short extension could be pulled out and then rapidly yanked as shown in Fig. 9. Difference images of these rapid and forceful deformations showed that only the actin within

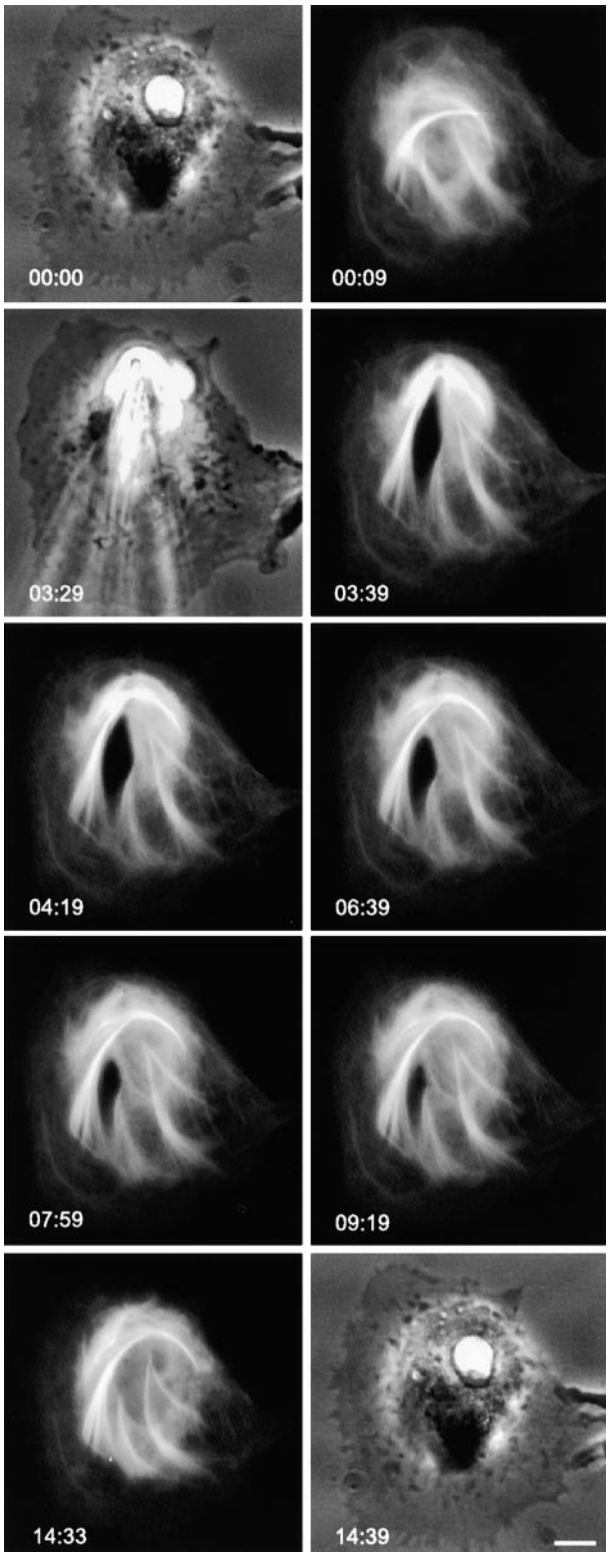

Figure 4. Viscoelastic behavior of microtubule bundles in GFP-MAP2c–transfected REF 52 cells (min:s). Bar, 20 μm. (00:00 and 00:09) Phase and fluorescent images of the cell before the cell was deformed. Note the shape and pattern of the three MT bundles in the perinuclear region. (03:29–03:39) Phase and fluorescent images of needle poked into the nuclear region of a cell, similar to Fig. 1. (04:19) Needle is held in position for ~1 min (tip of needle visible as white dot) and then released immediately after this frame. (06:39–14:39) MTs gradually recover and fill the space vacated by the needle. Note that after full recovery of nuclear shape, as seen in the phase images, the MT bundles remain deformed and displaced relative to initial conditions.

the short extension changed position (Fig. 9, lowest panels), the observable actin throughout the rest of the cell did not change position or shape.

Small experimentally induced extensions, as above, were observed to retract against even quite large tension loads imposed by a needle. In Fig. 10, a fibroblast transfected with GFP-MAP2c that was in the process of cell spreading (replated ~4 h before manipulation) was attached to the needle at the cell margin, which retreated and changed shape during the attachment process. After achieving attachment, the needle was pulled with gradually increasing force producing a short extension some 46 min after initial placement of the needle. By this time, the force in the extension was ~1,000 μdynes. Against this load, the cell spontaneously retracted the extension from 00:46 to 1:01 (h:min), shown as the difference between positions marked 1 and 1′ in the figure. Between 1:01 and 1:24, the applied tension was increased to ~3,000 μdynes and held. For the next 6 min, the cell again spontaneously retracted (difference between 2 and 2′ in the figure) against this significant force load. By 1:31 of this same experiment, the reference needle required to assess tension in the needle attached to the cell was at the very edge of the optical field. This was the maximum load we could measure at this magnification. Accordingly, we switched to the lowest available objective (10×) in order to increase the size of the optical field and raised the force to near 7,000 μdynes (see below). As before, the cell spontaneously retracted induced lengthening of the cellular process (data not shown). At this point, some 20 min after the sequence shown in Fig. 10, the reference needle had again been dragged to the edge of the optical field. To make an accurate measurement of force on the cell, we released adhesion of the cell to the calibrated needle by adding 60 μl of 0.5 mM EDTA in the vicinity of the needle tip allowing the needle to spring back to its zero-force distance. Based on the elastic recovery of a 16 μdyne/μm needle across 450 μm of the optical field, we estimate the cell and its process were supporting 7,200 μdynes or 7.2×10^{-8} N. The diameter of this cell process varied between 2.3 and 3 μm at different times during this experiment. Accepting the largest diameter and a circular cross section gives an estimated stress of 10^5 dynes/cm^2 (= 0.1 bar = 1.5 psi), which is approximately an order of magnitude lower than the stress of a tetanically contracting skeletal muscle.

The behaviors of the MTs during process extension and retraction was of some interest. First, a small number of MTs appear to be present in the experimentally induced cell process of Fig. 10. More importantly, however, the images show very little change in the position or shape of the cell itself or of the nucleus. Further, there was little change in the prominent MT bundles seen within this cell. Particularly noteworthy is the bundle nearest the cone-shaped, mechanical anchor region of the experimentally induced extension. This bundle of MTs deformed very little throughout this sequence despite the substantial forces that are being exerted on a neighboring local region.

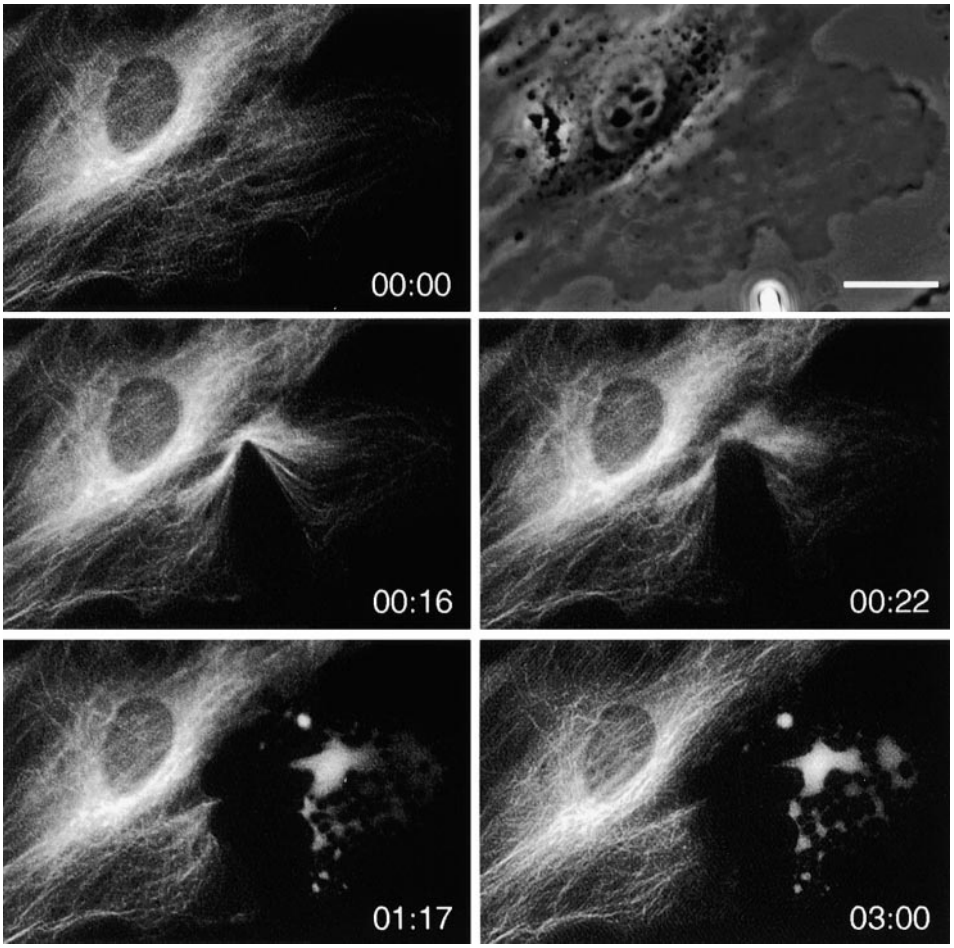

Figure 5. Response of GFP-tubulin–labeled microtubules to severing (min:s). Bar, 30 μm. (00:00) phase and fluorescent images taken immediately before poking with a broken needle. (00:16) Broken needle is forced into cell, where it appeared to act like scissors, i.e., cutting both from the top and bottom. (00:22) Needle just removed, note the MT array to the left of the cut. (01:17–03:00) Note that MT array to the left of the cut remains nearly unchanged, while the cell fragment to the left of the cut undergoes rapid and complete lysis.

Two types of control experiments were conducted for "towing" experiments using laminin-treated needles. Untreated needles (data not shown) were applied to the surface of the cell but never formed detectable attachments, nor was GFP-labeled actin observed to concentrate at the application site of such needles (or anywhere else). Needles were also treated with polylysine. These were found to stimulate recruitment of GFP–γ-actin to the site of the needle, albeit more slowly than for laminin-treated needles, and the connection was strong enough to permit "walking" of the actin accumulation across the cell surface (Fig. 11). However, these polylysine-mediated attachments were relatively weak, detaching at applied tensions between 100–200 μdynes ($1–2 \times 10^{-9}$ N).

Discussion

Two fundamentals for a mechanical understanding of any complex structure, e.g., a machine or a cell, are the mechanical behaviors of substructures composing the complex object and their interconnections. The development of GFP technology for cytoskeletal proteins (Ludin and Matus, 1998) enabled us to make some direct observations of the actin and MT cytoskeletons in response to applied mechanical forces. Our goal was not to examine the rheology of the cell in the usual sense of quantitative coefficients of fluid/solid stiffness, but to understand better the behaviors, e.g., the flow field, of the cytoskeleton and its interconnections in response to a variety of simple mechanical interventions. Indeed, these observations were most informative in assessing the time scale and spatial range over which the cytoskeleton changed or maintained form in response to forces that were of the same magnitude that these fibroblasts themselves exert. When a probe without attachment to the underlying cytoskeleton was used to apply force, we found that these attached cells behaved as predicted by the three-layer model of Dong et al. (1991). The cell appears as a highly elastic nucleus that is surrounded by cytoplasmic MTs that behave like a viscoelastic fluid (e.g., jelly). The third and outermost layer is an elastic cortical actin shell with a sustained tension (prestress in the actin structures). The stiffness of this layer increased markedly when the experimental needle was treated with laminin to recruit the actin cytoskeleton to the surface. By directly visualizing the actin recruitment, we confirmed a widely postulated model for mechanical connections between integrins and the actin cytoskeleton. Whether the probe applied simple deformations to the cell or interacted with the cytoskeleton, we found little evidence for strong connections between the actin cortex and linear elements of the cytoskeleton, either stress fibers or the underlying MT network. That is, we observed that experimentally applied forces produced unexpectedly local responses by the cytoskeleton. In this regard, we found no

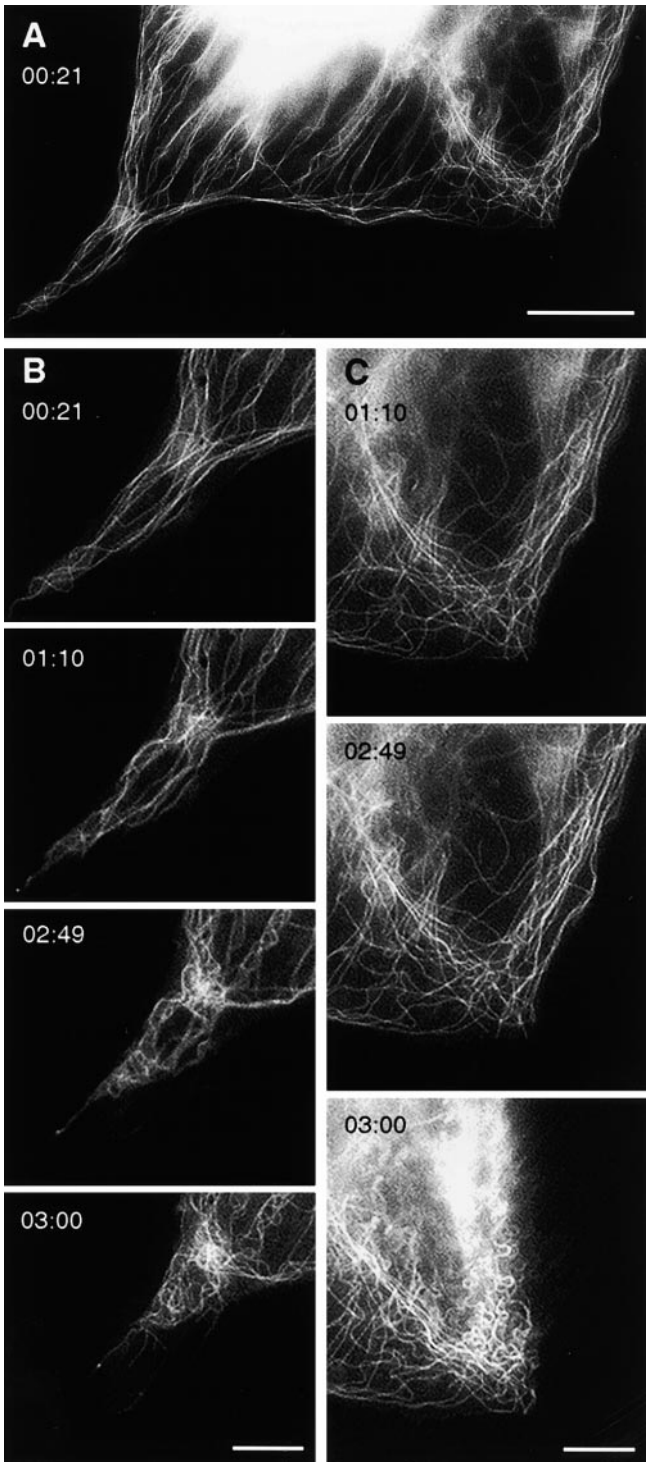

Figure 6. Microtubule buckling in GFP-tubulin–transfected cells undergoing rounding up in response to EDTA added to culture medium (min:s). (A) Lower magnification view of bottom portion of cell immediately after cell rounding became apparent. The narrow process extending from the cell at about 7 o'clock in shown at later times in panel B, while the right quadrant is shown at later times in panel C. Bar, 20 μm. (B) Higher magnification views of narrow cell extension during relatively rapid cell movement. Note that between 00:21 and 1:10 the MTs have moved ~5 mm and the MTs in the upper part of the process have substantially buckled. By 3:00 after the beginning of movement the cytoplasm has substantially retracted from the narrow process with clear buckling of essentially all MTs. (C) Higher magnification view of very rapid retraction of cytoplasm in right quadrant of the cell. Note that while the narrow cell extension on the left was retracting, this region of the cell remained quite stable for the first 3 min. But between 02:49 and 03:00, a catastrophic collapse of this region of cytoplasm occurs, with dramatic buckling of the MTs. Bars: (B and C) 10 μm.

evidence for a complementary force interaction between prestressed actin and compression-bearing MTs.

In one experimental series (Figs. 1–5), needles were used to poke, prod, and cut the cell while we observed the deformations of the actin and MT cytoskeleton. The nucleus was highly compliant and highly elastic; poking with a needle caused the nucleus to undergo substantial local deformations that recovered very rapidly after release of the needle (Fig. 1). The contribution of the nucleus to the deformability of the cell has received very little attention, e.g., no mention in several recent reviews and monographs on cytomechanics (Bereiter-Hahn et al., 1987; Elson, 1988; Ingber, 1997). Our observations suggest that the properties of the nucleus are likely to play a significant role in the mechanical responses of cells, particularly the central region of attached cells. As previously shown by Maniotis et al. (1997), we observed that the nucleus is stabilized in position by the actin cytoskeleton. Our observations did not allow us to determine whether this was by attachment or by steric entanglement, but movement of the nucleus clearly caused equivalent movements in the surrounding actin network, which also behaved elasticially (Fig. 1). Indeed, our results for the mechanical behavior of actin are entirely consistent with the well-established view of the cortex as being an elastic structure under sustained tension or prestress (Lewis, 1947; Bray and White, 1988; Hochmuth, 1993; Ingber, 1997). Actin observed in our transfected REF cells recovered its shape and position after noninjurious deformation over the course of seconds indicating nearly pure elasticity (Figs. 1 and 2). Sustained tension was clearly indicated by the behavior of actin to cutting, in which the severed actin bundle retracted strongly (Fig. 3) with most change again occurring over the course of seconds followed by only minor changes over the course of the following minutes. The sustained tension in the cortex is presumably balanced by positive fluid pressure in the cytoplasm, which also provides resistance to poking, but this appears not to be a large force in relation to cytoplasmic viscosity insofar as no cytoplasmic spillage followed any cutting intervention.

However, the high degree of localization of the actin response to pushing, prodding, and cutting was surprising given the widespread view of an integrated cytoskeletal network (Schliwa, 1986; Heidemann and Buxbaum, 1990; Forgacs, 1995; Ingber, 1997). By and large, only the actin filaments in the very immediate region of the intervention showed a response. These highly local responses to major changes in the form and/or connections of the cytoskeleton are inconsistent with complementary force interactions between tensile actin and compressed MTs, which would be predicted to promote more widespread rearrangements (Heidemann and Buxbaum, 1990; Ingber, 1997).

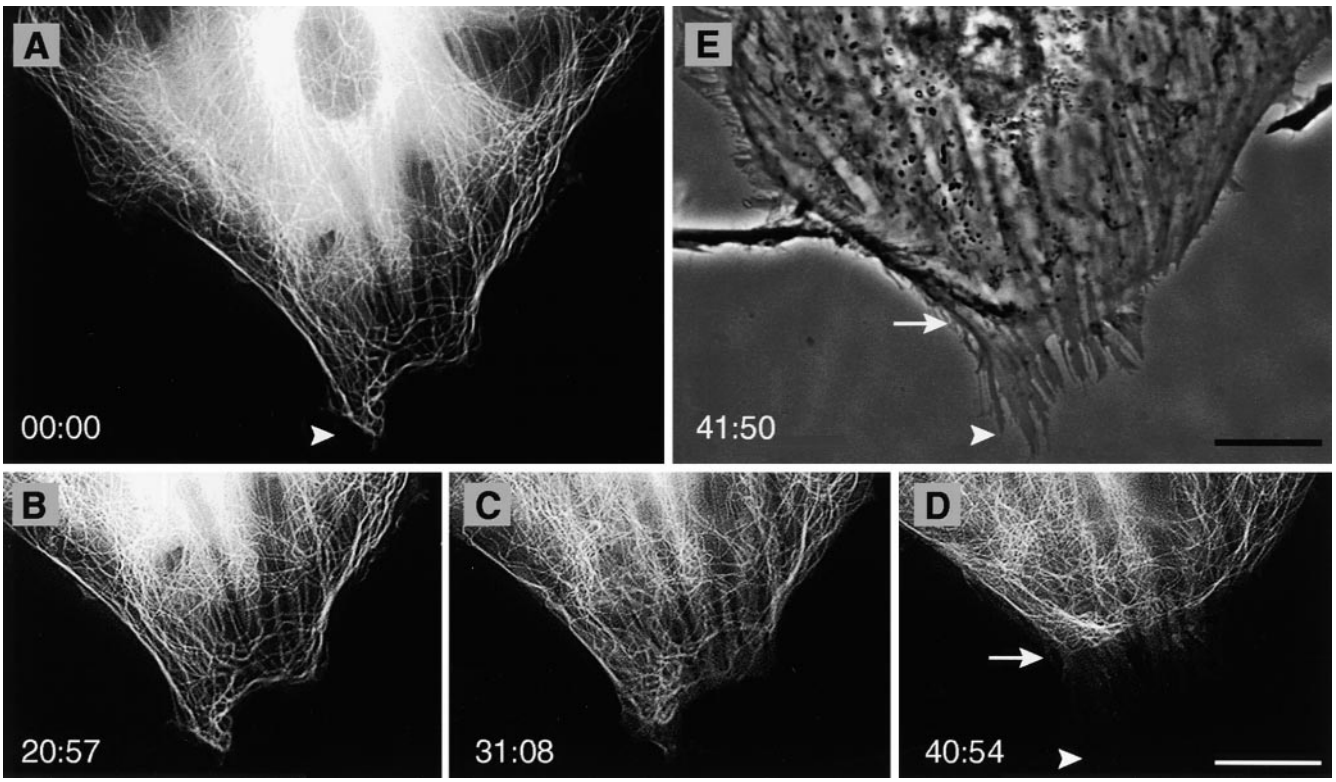

Figure 7. Microtubules undergoing shearing flow in GFP-tubulin–transfected cells undergoing rounding up in response to EDTA added to culture medium (min:s). Bars, 20 μm. (A) Fluorescent image of cell just before the addition of EDTA. Arrowhead shows initial terminus of MT-rich cytoplasm, which coincides with edge of cell. (B) 20 min later, the cell continues stable, note the number of MT "landmarks" that remain visible over this 20-min period, e.g., the relatively bright, thickenings of MT bundles at both left and right sides. Immediately after this frame, the MTs began a slow movement. (C) Over the next 10 min the cytoplasm has retracted ~7 mm, although some buckling is observable, most MTs have translocated. (D) Over the next 20 min, the MT-rich cytoplasm slowly retracted some 18 μm from its original position. Several MT landmarks have moved relative to the dish and relative to one another, although this is much more easily seen in the dynamic sequence. As seen, the arrow marks the edge of the retracted cytoplasm. (E) Phase image taken immediately after panel D, showing that the membranous margin of the cell has remained nearly stationary throughout (compare to panel A) while the MT-rich cytoplasm has sheared away inside this envelope as shown by the difference between the arrowhead and arrow.

In contrast to the elastic behavior of the nucleus and actin network, MTs behaved as a viscoelastic fluid and we observed little evidence for tethering among MTs or between MTs and the overlying cortex. That is, rapid deformations produced elastic, solid behaviors while deformations on a longer time scale produced flow and permanent deformations. The most dramatic solid-like behavior of MTs occured when they buckled in response to rapid retractions of cellular regions where the MTs were arrayed axially to the direction of retraction (Fig. 6) but even this buckling could result from cytoplasmic flow around floating MTs (e.g., like noodles in stirred soup). In all instances of buckling, no evidence for compression-induced MT disassembly was noted, although continued dynamic instability was observed. This suggests that either there was no compressive force on MTs, or that force does not directly regulate assembly/disassembly of MTs (Buxbaum and Heidemann, 1988, 1991), at least in fibroblasts. Because the buckling of MTs began almost immediately on cytoplasmic retraction, i.e., when the compressive force would seem to be not much greater than before retraction, we suggest that the ability of fibroblast MTs to bear a compressive load is quite weak. Nor did we ever observe a concerted or organized shift in the MT array suggestive of an integrated arrangement of MTs that distributed an increased compressive load throughout the array. Instead there was only random buckling and on even a slightly longer time scale (min), MTs showed clear fluid behaviors. In the relatively slow cellular retraction of Fig. 7, MTs primarily flowed past one another rather than buckled to accomodate the cytoplasmic movement. Even the MAP-induced bundle of MTs of Fig. 4, where bundling would be expected to increase any elastic stiffness, showed only partial recovery of deformation. When MT bundles were manipulated directly by the needle, the bundles moved differently indicating a lack of interconnection, and were deformed in shape and position over the time scale of 10 min, dramatically different from the elastic recovery within seconds for actin responses. In rounding cells at the beginning of the formation of retraction fibers (Harris, 1973), the MT cytoskeleton retracted independently of the overlying cortex, which remained attached at the same sites on the substratum (Fig. 7, D and E) indicating a lack of interconnection between the MTs and actin cortex.

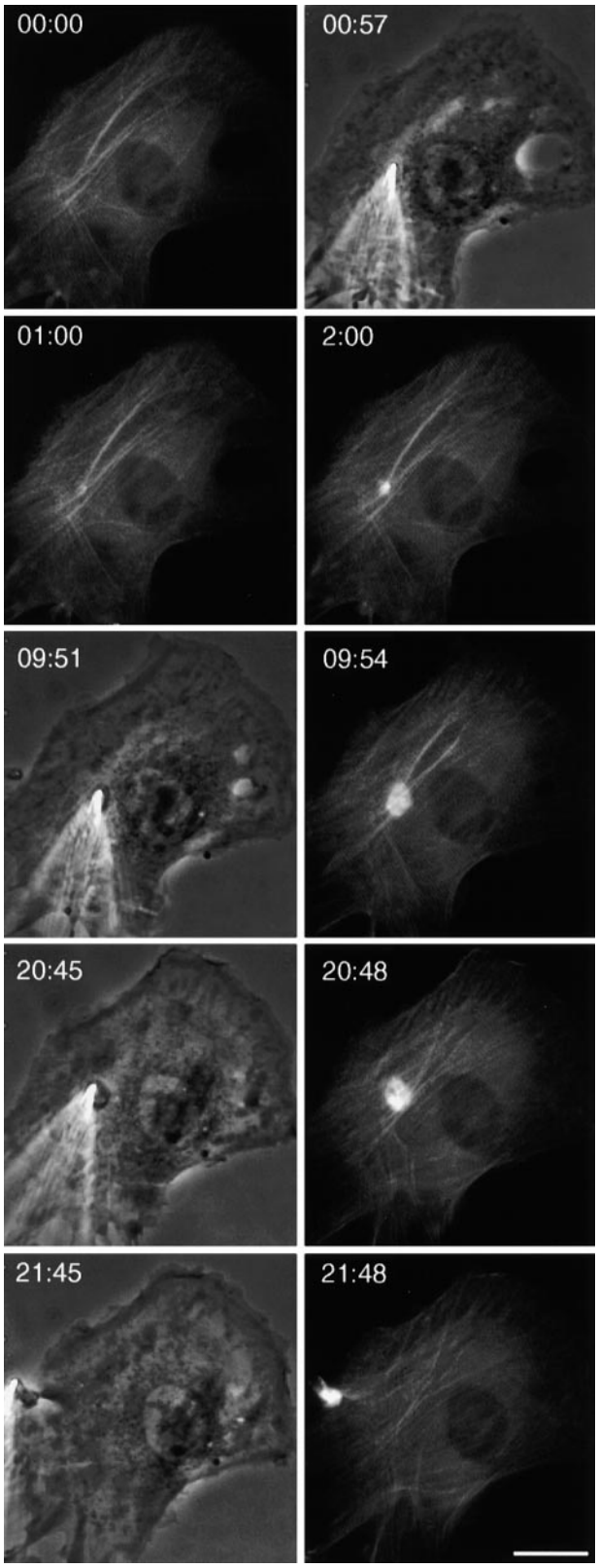

Figure 8. Recruitment of cortical actin by laminin treated needle in GFP–γ-actin–transfected cell and its subsequent towed movement (min:s). Bar, 30 μm. Cell just before application of needle (00:00) to "dorsal" surface of cell as seen in phase in 00:57. By 1:00, fluorescently labeled actin begins to increase in concentration directly beneath the tip of the needle, and continues increasing in concentration there over ~10 min (9:51 and 9:54). Leftward force is exerted by the needle between 10 min and ~20 min, eventually translocating the recruited actin to the edge of the cell where a short extension begins forming. Subsequent elongation and yanking on this extension in shown in Fig. 9.

When large numbers of MTs were severed in a spread cell (Fig. 5), there was little or no long-range response. The cytoplasm at the cut edge of the living fragment behaved as if one had used a knife to cut through agar. We note that the rapid lysis of the severed fragment shown in Fig. 5 indicates that, except in this case, our manipulations did not significantly damage the experimental cells. Thus the responses of the cytoskeleton we observed cannot be ascribed to necrotic events. Indeed, cells are known to survive mechanical insult rather well, due in part to the capacity of the plasma membrane to reseal rapidly (McNeil and Steinhardt, 1997). Our results suggest that the localized mechanical responses of the cytoskeleton may also make an important contribution to injury resistance, e.g., the lack of wound spreading in Fig. 3 despite the cortical tension.

This simple three-layer behavior for the "passive" rheology of the cell became more complex and active when the needle was treated with laminin and used to recruit actin to the cell surface, presumably through integrins (Ingber, 1991; Hynes, 1992; Yamada and Miyamoto, 1995; Burridge et al., 1997). Actin remained elastic in these experiments, but seemed more like a rigid, solid gel than like the relatively compliant cellular structure seen with untreated needles. It is clear from Figs. 8–10 that laminin-treated needles form strong attachments to the cell surface and the actin array, but despite the application of substantial forces, the deformation of the cell and cytoskeleton were both very local. In Fig. 10, the cell retained its locally deformed shape in the face of maintained and actively generated forces for a time scale of 100 min, as expected for rigid solids. We observed no integrated, wide-spread changes in the position of cytoskeletal or other cellular components. In the examples shown in Figs. 9 and 10, pulling on the cell margin caused only a local change in cell shape, the formation of a cellular process. Neither the actin nor the MTs in regions neighboring the extension were altered by changes in the length or position of the extension itself nor did the cytoskeletal filaments in these regions show significant responses to changes in the forces exerted nearby. Again, these behaviors and their time scale suggests the sort of viscoleastic behavior typical of rigid solids, i.e., pulling produces only local necking without long range structural rearrangement.

We presume that the contractions we observed by the experimentally induced cell processes (Fig. 10) are actomyosin-based contractions of the cortex, roughly similar to the well-described contraction of fibroblasts in collagen gels (Grinnell and Lamke, 1984) and on deformable growth substrata (Stopak and Harris, 1982). The largest force we measured in this example was consistent with a recent measurement of the force generated by fibroblasts during locomotion (Galbraith and Sheetz, 1997) and with contractile force exerted by essentially spherical fibroblasts (Thoumine and Ott, 1997). The stress across the induced cellular process was similar to that of fibroblasts

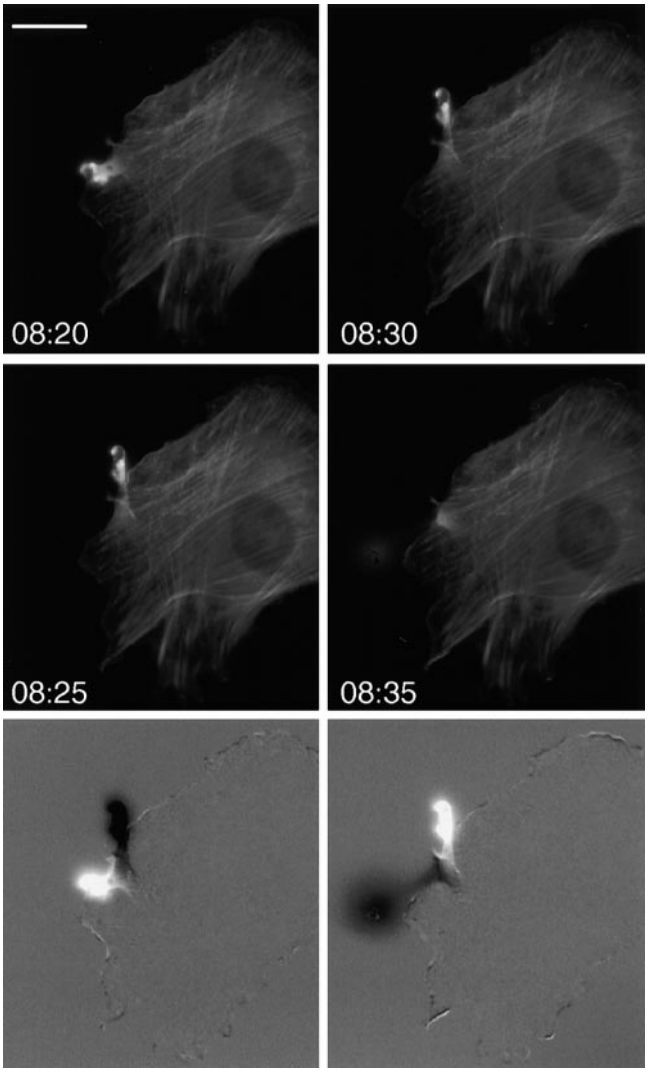

Figure 9. Rapid deformation of induced cellular extension in the same GFP–γ-actin–transfected cell as shown in Fig. 8 (min:s). Bar, 30 μm. The short extension induced by a laminin-treated needle as shown in Fig. 8 was lengthened by towing with the needle for an additional 8 min (needle moved to the left of the optical field) at which point two rapid, successive pulls (08:20–08:25 and 08:30–08:35) on the extension were made perpendicular to the towing direction (needle moved toward and away from the observer) between 8:20 and 8:35. Beneath each pair of fluorescent images is a difference image showing the pixel subtraction difference for each pull. Note that only the actin in the extension moves, the actin throughout the rest of the cell has remained essentially stationary.

strongly stimulated to contract with thrombin (Kolodny and Wysolmerski, 1992). In sharp contrast to cultured neurons that show a fluid-like growth response to tension and contract when slackened (Heidemann and Buxbaum, 1990; Chada et al., 1997), fibroblasts responded to experimental extension with contractions of increasing force. We think it likely that by experimentally applying forces with laminin-treated needles, we engaged adhesion, deformation-sensing, and tensile-response machinery normally engaged in the wound-closure function of fibroblasts (Grinnell, 1994).

We found the events of needle attachment interesting of themselves, although we can provide only a preliminary and incomplete interpretation. First, we observed a local accumulation of actin in the cytoplasmic region corresponding directly with the extracellular site of the laminin, an important ligand for integrins. This lends support to a widely accepted model of integrin-mediated attachment: that ligand binding to integrins causes a mechanical connection to the underlying cytoplasmic actin network (Ingber, 1991; Yamada and Miyamoto, 1995; Burridge et al., 1997). We were nevertheless surprised by the rapidity with which a visually dramatic accumulation of actin occurred and the strength of the connection between laminin and the cell surface. The adhesion between the cell and the tip of the needle shown in Fig. 10 was demonstrated to bear forces on the order of 10^{-8} N for >1 h. There is no reason to assume that this represesents the upper limit of adhesive force, rather it was the largest force we could measure under the experimental circumstances. Intriguingly, the cortical actin accumulation at the needle could be dragged across the cell with only modest forces, again suggesting a lack of strong connections between the actin cortex and the underlying cytoplasm. The ability to pull out cellular extensions with larger forces indicates that under some conditions the connections between the extracellular adhesion protein (i.e., laminin) and the actin cortex are quite strong, e.g., able to resist stresses ~1/10 that of contracting muscle. In this regard, Choquet et al. (1997) have shown that tension increases the strength of cytoskeletal connection to integrin receptors at lower forces ($\sim 10^{-11}$ N) and it may be that similar stress hardening occurred during our interventions. However, these tentative conclusions will require further study as the mechanical aspects of cellular attachment are currently less well understood than the underlying chemistry.

In control experiments for laminin-treated needles, we found that polylysine-treated needles, but not untreated needles, also caused an accumulation of actin that was capable of being translocated beneath the cell surface. However, the attachment was not nearly as strong as with laminin. Cytoskeletal involvement and the architecture of polylysine-mediated adhesion has not received much attention, presumably because polylysine is a nonphysiological, nonspecific adhesion protein. Our results suggest that polylysine also causes actin assembly beneath the surface site of adhesion. With our method of applying tension, however, polylysine-mediated adhesion was considerably weaker, we would estimate by an order of magnitude, than laminin-integrin adhesion.

Our results are difficult to reconcile with a tensegrity model of the cell in which sustained tension in the actin network is supported in part by compression of underlying MTs (Heidemann and Buxbaum, 1990; Ingber, 1997). Nor do our data provide any support for the related but separate idea that such a complementary force interaction directly regulates MT assembly/disassembly dynamics, at least in fibroblasts (Buxbaum and Heidemann, 1988; Kaech et al., 1996). As implied by the origin of its name, tensegrity structures are those in which the tensional elements behave in an integral fashion to provide the large-

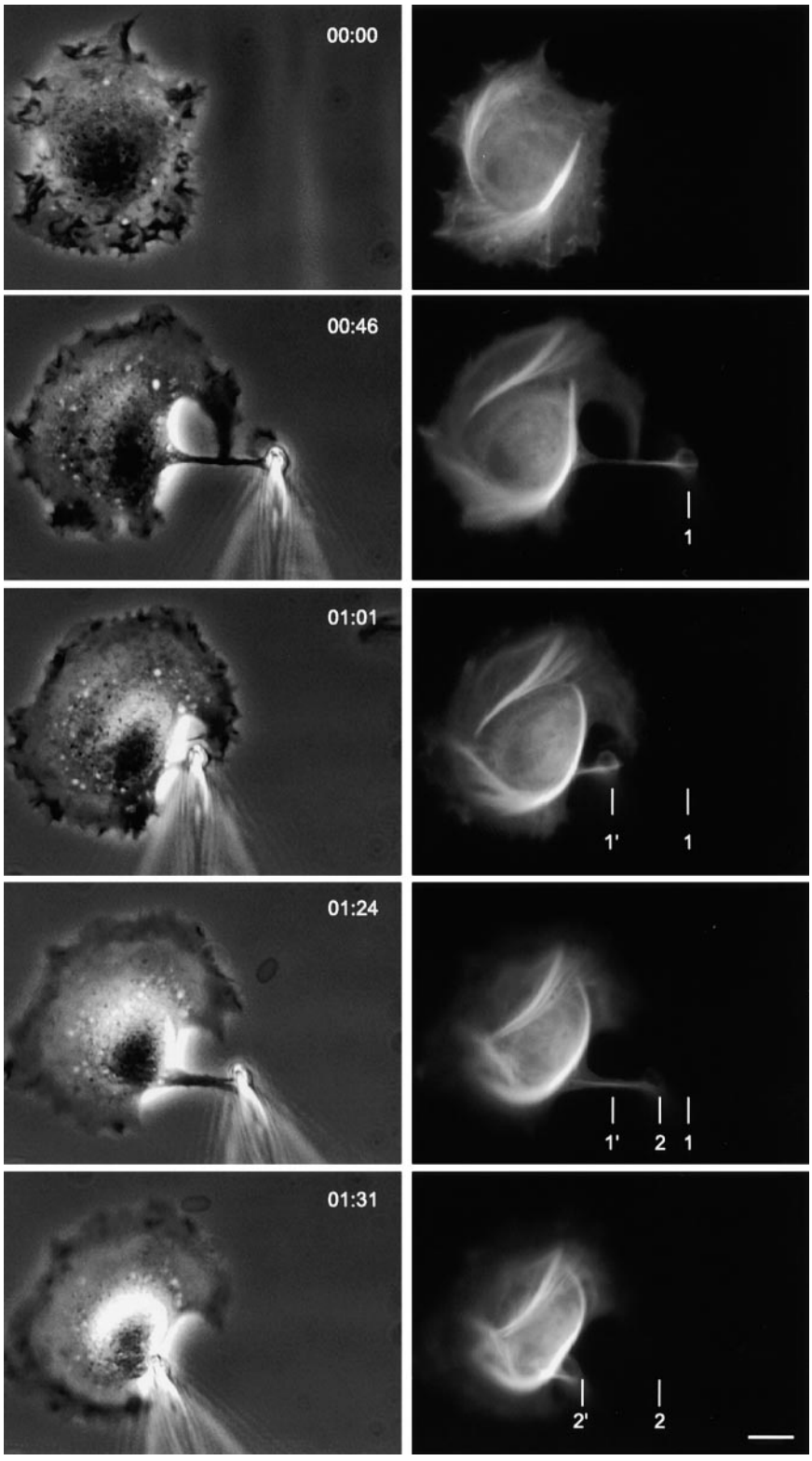

Figure 10. Forceful spontaneous retraction of experimentally induced cellular extension in GFP-MAP2c–transfected cell manipulated with a laminin-treated needle (h:min). Bar, 15 μm. Cell is shown before application of needle in fluorescent and phase images of 00:00. Over the next 40 min, a cellular extension is induced and pulled by a laminin-treated needle, essentially by the same process shown in Figs. 8 and 9. By 00:46, experimental movement of the needle had stopped and the length of process extension is shown by the mark labeled "1." Over the next 15 min, this extension spontaneously retracted against the load of the needle (~1,000 μdynes), shortening its length to 1′ by 01:01. Subsequently, the extension was experimental towed to the right increasing in length to position 2 by 01:24. At 1:24 experimental towing was again halted, and the extension spontaneously retracted against this load (~3,000 μdynes), shortening to position 2′. The presence of an increasing force load on the cell extension can be seen by the change in the angle of the needle during the experiment. Note the high stability of the shape and position of the MT array in the cell.

scale shape of the structure; i.e., tension creates large-scale integrity (Fuller, 1961). Classic tensegrity structures also involve intimate and distributed connections between the overlying tensile network and internal compressive struts so that changes in the network produce changes in the array of struts. Yet we repeatedly observed that both the actin- and MT-based cytoskeleton responded only locally to either passive deformations or those in which the needle was attached to the actin cytoskeleton. In view of the direct evidence that some of the actin-based tension is borne by attachments to the dish (e.g., cells round up when detached from it), if MTs were compression-bearing ele-

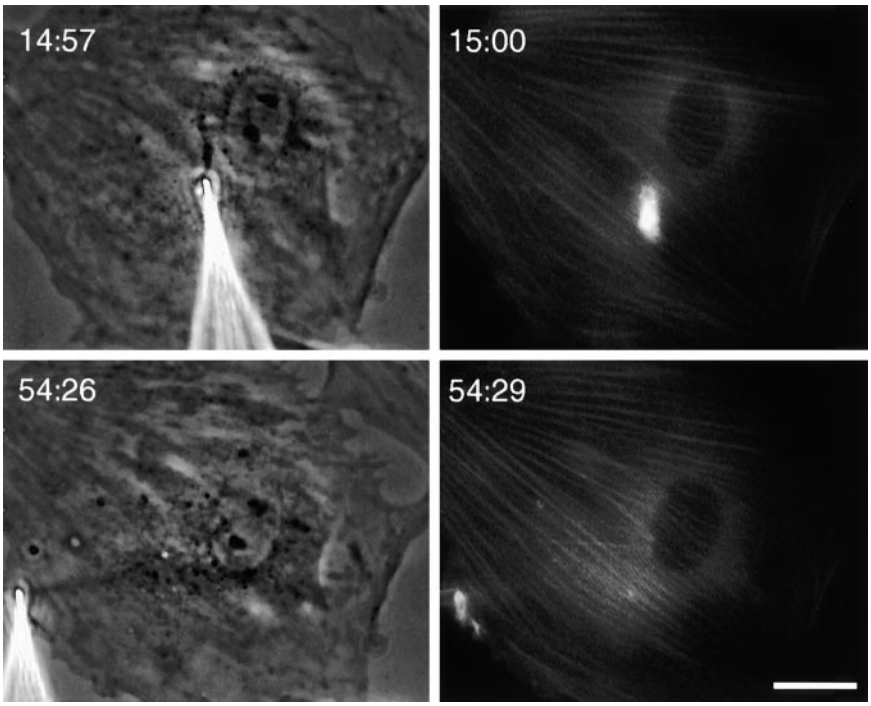

Figure 11. Recruitment of cortical actin by polylysine treated needle in GFP–γ-actin–transfected cell and its subsequent towed movement (min:s). Bar, 30 μm. Essentially similar to Fig. 8 except that the needle in this case had been treated with polylysine and applied to the top surface of the cell. As shown here, within 15 min of needle application, fluorescent actin has accumulated beneath the tip of the needle. With slow towing at modest forces, this actin accumulation was walked across the top surface of the cell to the cell margin over the next 40 min. However, increased tension at this time in an effort to elongate an extension caused the cell to release from the needle.

ments in fibroblasts, then relatively rounded cells would tend to have more compressive force supported by MTs and the cortex would be more likely to bear on the MTs. For this reason, we manipulated both well-spread cells (Figs. 2, 3, 5–9, and 11) and cells that had been replated 2–6 h earlier and so were relatively rounded and in the process of forming strong attachments (Figs. 1, 4, and 10). We observed no differences in the cytoskeletal behaviors of rounded cells or well-spread cells in response to manipulation. Regardless of apparent degree of spreading and presumably attachment, the cytoskeletal responses to deformation were surprisingly local. In this regard, Thoumine and Ott (1997) conducted rheological measurements on essentially spherical chick embryo fibroblasts. Although no cytoskeletal inferences could be drawn, the overall behavior of their highly rounded cells were entirely similar to those reported here for fibroblasts of varying degrees of spreading: highly elastic responses over the time scale of seconds, viscoelastic responses over 5–15 min, and an active contractile response with adhesive conditions. In aggregate, these results indicate that fibroblasts do not change their qualitative, and possibly quantitative, mechanical properties depending on their shape or degree of spreading, as would be predicted of a tensegrity structure.

The use of GFP-technology to visualize the cytoskeleton of living cells in real time adds an additional dimension to cellular rheology and cytomechanics. This technology makes it possible to directly observe the behaviors and interconnections of cytoskeletal elements in response to changes in cell shape and activity. We hope to exploit this technology in the future to better understand the cytoskeletal mechanics underlying cell crawling and the slower changes of cell shape change.

We thank Phillip Lamoureux for expertly providing the large numbers of calibrated glass needles required for this study and David Mooney, Donald Ingber, and Fred Grinnell for stimulating discussions. Finally, S.R. Heidemann is most grateful to the members of the Matus lab for hospitality above and beyond the call of sanity.

We thank the Human Frontiers Science Program Organization (Strasbourg, France) for a Short Term Fellowship (S.R. Heidemann), which made this collaboration possible. This work was also supported by the Friedrich Miescher Institute and by a grant (S.R. Heidemann) from the National Science Foundation (IBN 9603640).

Received for publication 22 October 1998 and in revised form 3 March 1999.

References

Adams, D.S. 1992. Mechanisms of cell shape change: the cytomechanics of cellular respone to chemical environment and mechanical loading. *J. Cell Biol.* 117:83–93.

Bereiter-Hahn, J., O.R. Anderson, and W.E. Reif. 1987. Cytomechanics. Springer Verlag, Berlin.

Bray, D., and J.G. White. 1988. Cortical flow in animal cells. *Science.* 239:883–888.

Burridge, K., M. Chrzanowska-Wodnicka, and C. Zhong, 1997. Focal adhesion assembly. *Trends Cell Biol.* 7:342–347.

Buxbaum, R.E., T. Dennerll, S. Weiss, and S.R. Heidemann. 1987. F-actin and microtubule suspensions as indeterminate fluids. *Science.* 235:1511–1514.

Buxbaum, R.E., and S.R. Heidemann. 1988. A thermodynamic model for force integration and microtubule assembly during axonal elongation. *J. Theor. Biol.* 134:379–390.

Buxbaum, R.E., and S.R. Heidemann. 1992. An absolute rate theory model for tension control of axonal elongation. *J. Theor. Biol.* 155:409–426.

Chada, S., P. Lamoureux, R.E. Buxbaum, and S.R. Heidemann. 1997. Cytomechanics of neurite outgrowth from chick brain neurons. *J. Cell Sci.* 110:1179–1186.

Choquet, D., D.P. Felsenfeld, and M.P. Sheetz. 1997. Extracellular matrix rigidity causes strengthening of integrin-cytoskeletal linkages. *Cell.* 88:39–48.

Cleveland, D.W. 1988. Autoregulated instability of tubulin mRNAs: a novel eukaryotic regulatory mechanism. *Trends Biochem Sci.* 13:339–343.

Dennerll, T.J., P. Lamoureux, R.E. Buxbaum, and S.R. Heidemann. 1989. The cytomechanics of axonal elongation and retraction. *J. Cell Biol.* 109:3073–3083.

Dong, C.R., R. Skalak, and K.-L.P. Sung. 1991. Cytoplasmic rheology of passive neutrophils. *Biorheology.* 28:557–567.

Elson, E.L. 1988. Cellular mechanics as an indicator of cytoskeletal structure and function. *Annu. Rev. Biophys. Biophys. Chem.* 17:397–430.

Evans, E., and A. Yeung. 1989. Apparent viscosity and cortical tension of blood granulocytes determined by micropipet aspiration. *Biophys. J.* 56:151–160.

Ferry, J.D. 1959. Rheology of macromolecular systems. *In* Biophysical Science, A Study Program. J.L. Oncley, F.O. Schmitt, R.C. Williams, M.D. Rosenberg, and R.H. Bolt, editors. J. Wiley and Sons, New York. 130–135.

Fischer, M., S. Kaech, D. Knutti, and A. Matus. 1998. Rapid actin-based plasticity of dendritic spines. *Neuron.* 20:847–854.

Forgacs, G. 1995. On the possible role of cytoskeletal filamentous networks in intracellular signaling: an approach based on percolation. *J. Cell Sci.* 108: 2131–2143.

Fuller, R.B. 1961. Tensegrity. *Portfolio and Artnews Annual.* 4:112–127.

Galbraith, C.G., and M.P. Sheetz. 1997. A micromachined device provides a new bend on fibroblast traction forces. *Proc. Natl. Acad. Sci. USA.* 94:9114–9118.

Grinnell, F. 1994. Fibroblasts, myofibroblasts, and wound contraction. *J. Cell Biol.* 124:401–404.

Grinnell, F., and C.R. Lamke. 1984. Reorganization of hydrated collagen lattices by human skin fibroblasts. *J. Cell Sci.* 66:51–63.

Harris, A.K. 1973. Location of cellular adhesions to solid substrata. *Dev. Biol.* 35:97–114.

Heidemann, S.R., and R.E. Buxbaum. 1990. Tension as a regulator and integrator of axonal growth. *Cell Motil. Cytoskel.* 17:6–10.

Heidemann, S.R., P. Lamoureux, and R.E. Buxbaum. 1999. Mechanical stimulation of neurite assembly in cultured neurons. *In* The Neuron in Tissue Culture. L.W. Haynes, editor. John Wiley and Sons Ltd., London. 105–119.

Hochmuth, R.M. 1993. Measuring the mechanical properties of individual human blood cells. *J. Biomech. Eng.* 115:515–519.

Hynes, R.O. 1992. Integrins: versatility, modulation and signaling in cell adhesion. *Cell.* 69:11–25.

Ingber, D.E. 1991. Integrins as mechanochemical transducers. *Curr. Opin. Cell Biol.* 3:841–848.

Ingber, D.E. 1997. Tensegrity: the architectural basis of cellular mechanotransduction. *Annu. Rev. Physiol.* 59:575–599.

Kaech, S., B. Ludin, and A. Matus. 1996. Cytoskeletal plasticity in cells expressing neuronal microtubule-associated proteins. *Neuron.* 17:1189–1199.

Kolodney, M.S., and R.B. Wysolmerski. 1992. Isometric contraction by fibroblasts and endothelial cells in tissue culture: a quantitative study. *J. Cell Biol.* 117:73–82.

Janmey, P.A., S. Hvidt, J. Kas, D. Lerche, A. Maggs, E. Sackmann, M. Schliwa, and T.P. Stossel. 1994. The mechanical properties of actin gels: Elastic modulus and filament motions. *J. Biol. Chem.* 269:32503–32513.

Lamoureux, P., J. Zheng, R.E. Buxbaum, and S.R. Heidemann. 1992. A cytomechanical investigation of neurite growth on different culture surfaces. *J. Cell Sci.* 118:655–661.

Lewis, W.H. 1947. Mechanics of invagination. *Anat. Rec.* 97:139–156.

Ludin, B., S. Kaech, and A. Matus. 1996. Application of novel vectors for GFP-tagging of proteins to study microtubule-associated proteins. *Gene.* 173:107–111.

Ludin, B., and A. Matus. 1998. GFP illuminates the cytoskeleton. *Trends Cell Biol.* 8:72–77.

Maniotis, A.J., C.S. Chen, and D.E. Ingber. 1997. Demonstration of mechanical connection between integrins, cytoskeletal filaments, and nucleoplasm that stabilize nuclear structure. *Proc. Natl. Acad. Sci. USA.* 94:849–854.

Matus, A. 1994. MAP2. *In* Microtubules. J.S. Hyams and C.W. Lloyd, editors. Wiley-Liss, New York. 155–166.

McNeil, P., and R.A. Steinhardt. 1997. Loss, restoration, and maintenance of plasma membrane integrity. *J. Cell Biol.* 137:1–4.

Peterson, N.O., W.B. McConnaughey, and E.L. Elson. 1982. Dependence of locally measured cellular deformatbility on position on the cell, temperature and cytochalasin B. *Proc. Natl. Acad. Sci. USA.* 79:5327–5331.

Sato, M., W.H. Schwartz, and T.D. Pollard. 1987. Dependence of the mechanical properties of actin/actinin gels on deformation rate. *Nature.* 325:828–830.

Sato, M., T.Z. Wang, and R.D. Allen. 1983. Rheological properties of living cytoplasm: endoplasm of Physarum plasmodium. *J. Cell Biol.* 97:1089–1097.

Schliwa, M. 1986. The Cytoskeleton: An Introductory Survey. Springer-Verlag, Vienna. 145–178.

Stopak, D., and A.K. Harris. 1982. Connective tissue morphogenesis by fibroblast traction. I. Tissue culture observations. *Dev. Biol.* 90:38–54.

Stossel, T.P. 1993. On the crawling of animal cells. *Science.* 260:1086–1094.

Taylor, D.L., and J.S. Condeelis. 1979. Cytoplasmic structure and contractility in amoeboid cells. *Int. Rev. Cytol.* 56:57–144.

Thoumine, O., and A. Ott. 1997. Time-scale dependent viscoelastic and contractile regimes in fibroblasts probed by microplate manipulation. *J. Cell Sci.* 110:2109–2116.

Tran-Son-Tay, R., D. Needham, A. Yeung, and R.M. Hochmuth. 1991. Time-dependent recovery of passive neutrophils after large deformation. *Biophys. J.* 60:331–336.

Valberg, P.A., and D.F. Albertini. 1985. Cytoplasmic motions rheology and structure probed by a novel magnetic particle method. *J. Cell Biol.* 101:130–140.

Weisshaar, B., T. Doll, and A. Matus. 1992. Reorganization of the microtubular cytoskeleton by embryonic microtubule-associated protein 2 (MAP2c). *Development.* 116:1151–1161.

Yamada, K.M., and S. Miyamoto. 1995. Integrin transmembrane signaling and cytoskeletal control. *Curr. Opin. Cell Biol.* 7:681–689.

Zand, M.S., and G. Albrecht-Buehler. 1989. What structures, besides adhesions, prevent spread cells from rounding up? *Cell Motility Cytoskel.* 13:195–211.